HILL PUBLISHING

Theoretical Physics and Quantum Mechanics, 2025, 2(1), 11-21
https://www.hillpublisher.com/Journals/tpqm/
ISSN Online: 3066-5744

Gravitational Wave Analysis of Compact Binary Systems

Xiang Meng

International Department, Beijing No.80 High School, Beijing 100102, China.

How to cite this paper: Xiang Meng. (2025). Gravitational Wave Analysis of Compact Binary Systems. *Theoretical Physics and Quantum Mechanics*, 2(1), 11-21.
DOI: 10.26855/tpqm.2025.06.003

Received: September 7, 2025
Accepted: September 28, 2025
Published: October 31, 2025

***Corresponding author:** Xiang Meng, International Department, Beijing No.80 High School, Beijing 100102, China.

Abstract

Gravitational-wave astronomy has rapidly evolved into a transformative field, enabling direct observation of compact binary coalescences and providing unprecedented insights into the strong-field regime of general relativity. In this study, we analyze three confirmed events—GW170817, GW150914, and GW230627—using publicly available data from the LIGO Open Science Center. Through systematic signal processing, including whitening, bandpass filtering, and time–frequency analysis, we reproduce the characteristic "chirp" signatures of compact binaries and highlight the contrasting features of neutron star and black hole mergers. The long inspiral of GW170817 demonstrates the high-frequency evolution of binary neutron stars, while the shorter, lower-frequency chirps of GW150914 and GW230627 reflect the dynamics of more massive black hole binaries. By comparing time-domain, frequency-domain, and spectrogram representations, we confirm the astrophysical origin of these signals and their consistency with theoretical predictions. Our results underscore the accessibility of open data for scientific exploration and illustrate how even qualitative analyses can reveal the fundamental physics of compact binary systems.

Keywords

Gravitational wave; Compact binaries; Strain analysis; GWOSC

1. Background

Classical mechanics, developed in the 17th century by Isaac Newton and his contemporaries, provided a powerful framework for describing the motion of bodies under forces [1, 2]. For centuries it remained the dominant theory of physics [3], but its reliance on absolute concepts of space and time eventually proved insufficient in extreme regimes. Einstein's theories of special relativity [4] and general relativity [5, 6] replaced these abstractions with a covariant description of spacetime, in which gravity is understood as the curvature of spacetime itself. A natural consequence of this framework is the existence of gravitational waves (GWs): disturbances in spacetime generated by accelerating masses [7-9].

Indirect evidence for GWs came from the orbital decay of the Hulse–Taylor binary pulsar, which matched general relativity's predictions with remarkable precision [10]. The eventual di- rect detections by LIGO and Virgo transformed GWs from a theoretical prediction into a new observational tool, enabling the study of compact binaries, tests of general relativity, and even cos- mological measurements. Unlike electromagnetic radiation, which can be absorbed or scattered, GWs travel virtually unimpeded, carrying pristine information from otherwise inaccessible regions of the universe. This makes them a fundamentally new window on the cosmos.

2. Background

The starting point is Einstein's field equations,

$$R_{\mu\nu} - \frac{1}{2} g_{\mu\nu} R = \frac{8\pi G}{c^4} T_{\mu\nu},$$

where $R_{\mu\nu}$ is the Ricci curvature tensor, $g_{\mu\nu}$ is the metric tensor, scalar R describes spacetime curvature, and $T_{\mu\nu}$ represents energy and momentum. Together the equation relates the curvature of spacetime to the distributions of matter and energy, where. In the weak-field limit, we linearize the metric as

$$g_{\mu\nu} = \eta_{\mu\nu} + h_{\mu\nu}, \quad |h_{\mu\nu}| \ll 1,$$

leading to a wave equation for the perturbations $h_{\mu\nu}$ with the d'Alembertian operator $\Box$

$$\Box h_{\mu\nu} = -\frac{16\pi G}{c^4} T_{\mu\nu}.$$

Far from the source, the dominant contribution comes from the second time derivative of the mass quadrupole moment $I\left(t - \frac{r}{c}\right)$:

$$h_{ij}(t, r) = \frac{2G}{c^4 r} \ddot{I}\left(t - \frac{r}{c}\right)$$

This quadrupole formula shows that GWs are sourced by accelerated, non-spherically symmetric mass distributions. Compact binaries of black holes (BBHs) and neutron stars (BNSs) are therefore ideal emitters, producing the characteristic "chirp" signal as they inspiral and merge.

The luminosity carried away by GWs can be enormous. For a binary system near merger, the GW power output is on the order of

$$L_{\mathrm{GW}} \sim 10^{50}\ \mathrm{erg\ s^{-1}} \sim 10^{17} L_{\odot},$$

comparable to the combined luminosity of millions of galaxies.

Beyond individual detections, the field is now moving toward the study of the stochastic gravitational- wave background (SGWB). This background may arise from the superposition of unresolved astro- physical sources or from cosmological processes such as inflation, reheating, or first-order phase transitions. Its energy density spectrum is often expressed as

$$\Omega_{\mathrm{GW}}(f) = \frac{1}{\rho_c} \frac{d\rho_{\mathrm{GW}}}{d \ln f},$$

where ρ_c is the critical density of the universe. Measuring Ω_{GW} would provide a new probe of high-energy physics beyond the Standard Model.

Pulsar timing arrays (PTAs) have recently reported evidence for a common-spectrum stochastic signal, likely linked to supermassive black hole binaries. Meanwhile, ground-based interferometers such as LIGO and Virgo continue to detect stellar-mass binaries, and the planned space-based detector LISA will probe the millihertz band, sensitive to massive black hole binaries and galactic binaries [11].

Next-generation observatories will dramatically expand the reach of GW astronomy. The Einstein Telescope (ET) [12] and Cosmic Explorer (CE) [13] aim to detect essentially all stellar-origin black hole binaries in the observable universe, as well as tens of thousands of neutron star mergers per year (*14*). These observations will allow precise tests of general relativity, constraints on the equation of state of neutron stars, and independent measurements of the Hubble constant.

Space-based detectors such as LISA will complement this by targeting lower frequencies, enabling studies of the binary populations in the Milky Way (Galaxy), the growth of massive black holes, and potential cosmological backgrounds.

Together, these facilities will improve our understanding of gravitational waves. At the same time, the challenge of disentangling thousands of overlapping signals will require new data analysis strategies, including global parameter estimation and machine learning approaches.

3. Methodology

The methodology of this project combined theoretical study of gravitational-wave (GW) physics with hands-on analysis of publicly available data from the LIGO Open Science Center (LOSC). The aim sample to entire parameter space, but rather to qualitatively explore the signatures of compact binary coalescences in the time, frequency, and time–frequency domains. This section outlines the data acquisition, data processing, and analysis techniques.

3.1 Data acquisition

The primary data used in this study strain time series from the LOSC using Python from GWOSC, which provides open access to LIGO and Virgo observations. Specific events analyzed included well-known detections such as GW150914 (binary black hole merger) [15] and GW170817 (binary neutron star merger) [16]. These events represent the two most important classes of compact binary systems and have been extensively studied in the literature, providing a benchmark for comparison.

3.2 Data processing

The Raw interferometer strain data contain significant noise contributions from seismic, thermal, and quantum sources. We apply the processes below to enhance the signal-to-noise ratio.

3.2.1 Whitening

The detector noise spectrum is not flat: some frequencies dominate. Whitening divides the strain by the amplitude spectral density (ASD) of the noise, flattening the spectrum so that all frequencies contribute equally. This enhances the visibility of the GW signal.

```
Nt = len(strain)
white_hf = amps / (np.sqrt(interp_Pxx(freqs)))
white_ht = np.fft.irfft(white_hf, n=Nt)
```

3.2.2 Bandpass filtering

Compact binary signals are strongest in the ~ 20--2000 Hz range, where LIGO sensitivity is optimal. Frequencies outside this band are dominated by seismic noise (low-frequency) and shot noise (high-frequency). Applying a band-pass filter isolates the relevant frequency band.

```
fband = (20, 2000)
nyq = 0.5 * fs
low = fband[0] / nyq
high = fband[1] / nyq
b, a = butter(order, [low, high], btype='band')
normalization = np.sqrt((fband[1] - fband[0]) / (fs / 2))
white_ht_bp = filtfilt(b, a, data) / normalization
```

3.2.3 Windowing

To fix the abnormal frequency graph, we apply a Hann window to the time domain. This helps reduce spectral leakage of the frequency domain data.

```
n_samples = len(ldata)
window = get_window('hann', n_samples)
lwin = ldata * window
```

3.2.4 Segmentation for time-frequency domain analysis

To study how the frequency content evolves over time, the data must be divided into overlapping segments. Each segment is Fourier transformed, and the results are combined into a spectrogram. This helps reveal the inspiral, merger, and ringdown phases as a rising track in frequency.

```
spec = windowed_strain.spectrogram(fftlength=2, overlap=1)
spec.plot()
```

With these processing, the raw strain data are transformed into a form where the GW signal can be clearly identified in the time, frequency, and time--frequency domains.

3.3 Analysis domain

After processing, the strain data were analyzed in three complementary domains: time, frequency, and time–frequency. Each domain highlights different aspects of the gravitational-wave signal and connects directly to theoretical predictions from compact binary coalescences.

3.3.1 Segmentation for time-frequency domain analysis

To study how the frequency content evolves over time, the data must be divided into overlapping segments. Each segment is Fourier transformed, and the results are combined into a spectrogram. This helps reveal the inspiral, merger, and ringdown phases as a rising track in frequency.

3.3.2 Time domain

In the time domain, the whitened strain $h(t)$ is plotted as a function of time. For binary mergers, this reveals the characteristic ``chirp'' --- an oscillatory signal whose amplitude and frequency increase as the orbit shrinks. The signal terminates abruptly at the merger, followed by a short ringdown in some cases.

```
rel_times = ldata.times.value - gps
ax_time.plot(
rel_times,
ldata.value,
color='navy',
linewidth=0.7
)
```

3.3.3 Frequency domain

The frequency-domain view is obtained by Fourier transforming the strain to compute the amplitude spectrum using Fast Fourier Transformation (FFT). This representation highlights the dominant frequencies of the signal and allows comparison with theoretical predictions. More massive black hole binaries merge at lower frequencies, while less massive neutron star binaries chirp into higher frequencies.

```
fftamp = ldata.fft().abs()
freqs = fftamp.frequencies.value
amps = fftamp.value

ax_freq.loglog(
freqs,
amps,
color='darkred',
linewidth=0.7
)
```

3.3.4 Amplitude spectral density (ASD)

A more refined way to visualize the frequency content is through the amplitude spectral density (ASD), defined as the square root of the power spectral density (PSD). The ASD provides an estimate of the strain-equivalent noise of the detectors versus frequency, which limits their ability to identify GW signals.

```
fs = int(min(ldata.sample_rate.value,
hdata.sample_rate.value,
vdata.sample_rate.value))
NFFT = 4 * fs
Pxx_L1_hann, freqs_hann = mlab.psd(
strain_L1, NFFT=NFFT, Fs=fs,
window=np.hanning(NFFT),
noverlap=NFFT // 2,
detrend=mlab.detrend_none,
    scale_by_freq=True
)
    psd_L1_hann = interp1d(freqs_hann, Pxx_L1_hann,
    kind='linear',
    bounds_error=False,
    fill_value='extrapolate')
    asd_L1_hann = np.sqrt(psd_L1_hann(f_grid))
```

3.3.5 Time-frequency domain: spectrogram

To study how the frequency content evolves over time, the data must be divided into overlapping segments. Each segment is Fourier transformed, and the results are combined into a spectrogram. This helps reveal the inspiral, merger, and ringdown phases as a rising track in frequency.

```
spec = ldata.spectrogram2()**0.5
times_min = (spec.times.value - ref_gps) / 60.0
freqs = spec.frequencies.value
amp = spec.value

fig, ax = plt.subplots(figsize=(10, 6))
pcm = ax.pcolormesh(
times_min,
freqs,
    amp.T,
shading='auto',
    cmap=cmap,
    norm=LogNorm(vmin=1e-24, vmax=1e-20)
    )
```

3.3.6 Q-transformation

To zoom in on the chirp signal, a Q-transform can be applied. This method provides a time--frequency representation optimized for signals with varying frequency content, such as compact binary mergers.

```
qmap = h1.q_transform(frange=(30, 500))
times = qmap.times.value - gps
freqs = qmap.frequencies.value
energy = qmap.value
```

The Q-transformation highlights the inspiral track with greater clarity, making it easier to identify the gradual frequency increase leading up to merger.

3.4 Limitations

Our research is limited to qualitative analysis. Nevertheless, the methodology illustrates how theoretical concepts from general relativity manifest directly in observational data, and how even basic signal processing can reveal the physics of compact binaries.

4. Results

In this section, we present the results of our gravitational-wave data analysis. We begin with GW170817, the binary neutron star merger, before turning to the binary black hole event GW150914 and event GW230627. Each figure is accompanied by a brief explanation of its significance.

4.1 GW170817: binary neutron star merger

We begin our analysis of GW170817 by examining the signal in the time and frequency domains. Figure 1 shows the raw strain data. In the time domain, the oscillations increase in both amplitude and frequency, producing the characteristic ``chirp'' expected from a binary neutron star inspiral. In the frequency domain, the signal power is concentrated in the ~20-2000 Hz band, consistent with the expected range for neutron star mergers.

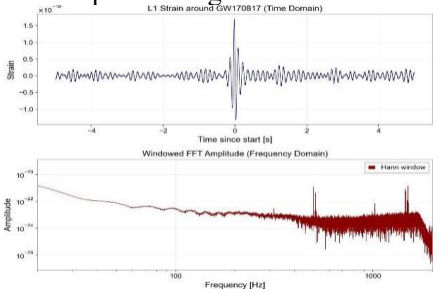

Figure 1. Time- and frequency-domain strain of GW170817.

The chirp is visible in the time series, while the frequency spectrum shows power concentrated in the most sensitive band of the detector. To place this in the context of detector sensitivity, Figure 2 shows the amplitude spectral density (ASD) of the Livingston detector around the time of GW170817. The ASD represents the strain-equivalent noise floor as a function of frequency. The signal lies within the most sensitive band, between ~

20-2000 Hz, which explains why the inspiral is clearly visible in subsequent analyses.

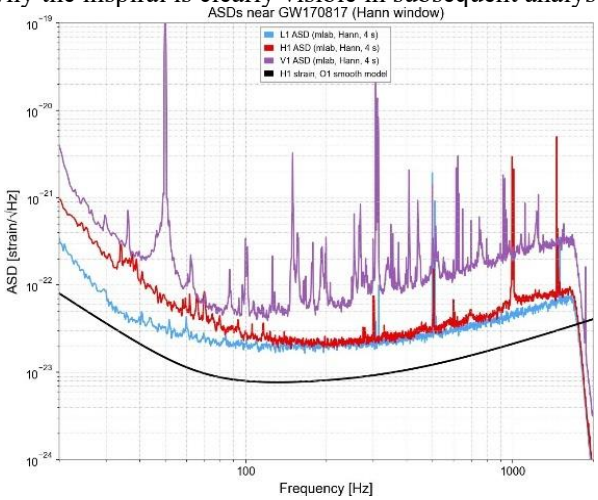

Figure 2. Amplitude spectral density (ASD) of GW170817.

After whitening the data to flatten the noise spectrum, the chirp becomes even clearer. Figure 3 shows the whitened strain in the time domain, where the increasing frequency and amplitude of the inspiral are evident.

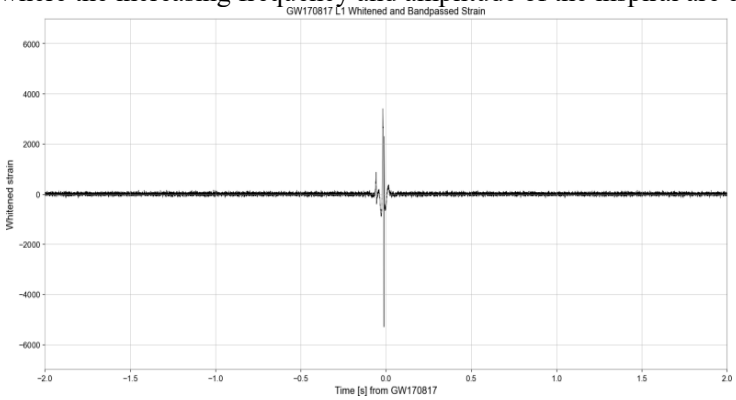

Figure 3. Amplitude spectral density (ASD) of GW170817.

A more complete picture is obtained in the time--frequency domain. Figure 4 shows the spectrogram of the raw data, while Figure 5 shows the whitened spectrogram. In both cases, the rising track corresponds to the inspiral, culminating in the merger. The whitened version enhances the visibility of the signal against the noise background.

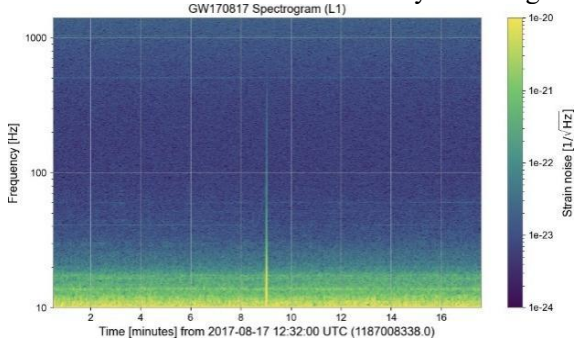

Figure 4. Time--frequency spectrogram of GW170817.

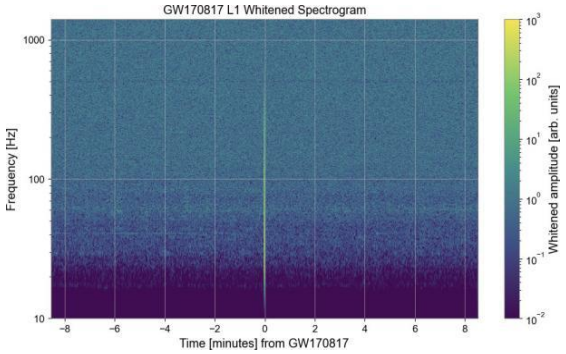

Figure 5. Whitened time--frequency spectrogram of GW170817.

Finally, Figure 6 shows the Q-transform of GW170817. This method provides a high-resolution time--frequency representation, making the chirp track especially clear.

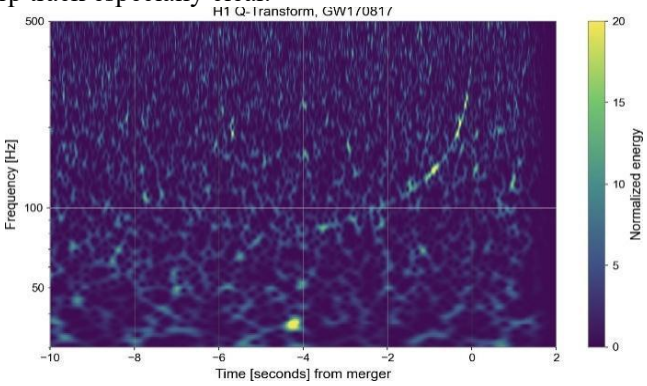

Figure 6. Whitened time--frequency spectrogram of GW170817.

Beyond visual inspection, we also performed matched filtering of GW170817 against templates from other events. Figures 7-9 show the matched filter outputs using templates from GW150914, GW151226, and GW170104, respectively. In each case, the correlation peaks at the time of the event, confirming the presence of a chirp.

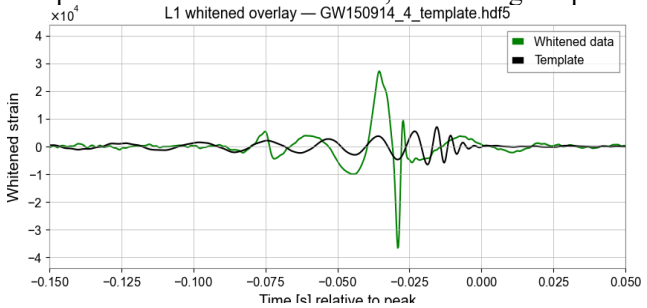

Figure 7. Matched filtering of GW170817 with the GW150914 template.

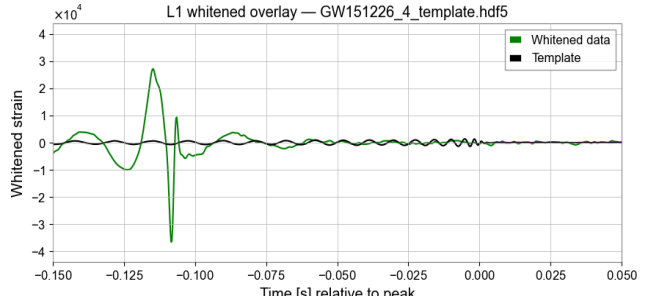

Figure 8. Matched filtering of GW170817 with the GW151226 template.

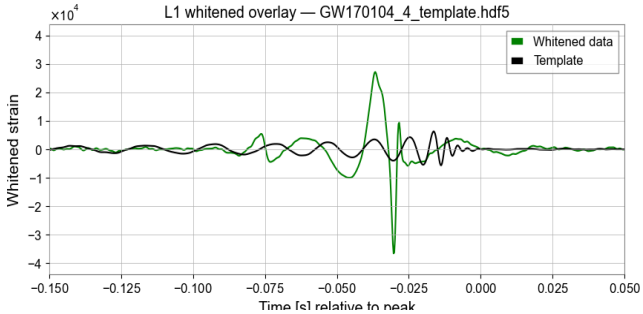

Figure 9. Matched filtering of GW170817 with the GW170104 template.

The corresponding signal-to-noise ratio (SNR) time series are shown in Figures 10-12. In each case, the SNR peaks at the merger time, consistent with the detection of a binary neutron star inspiral.

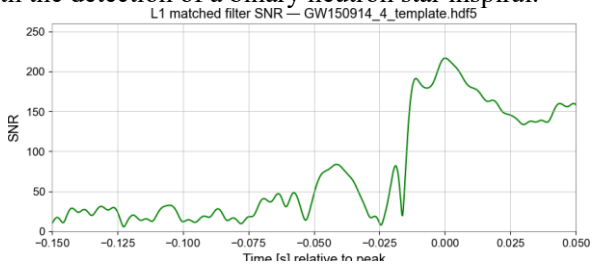

Figure 10. SNR time series for GW170817 using the GW150914 template.

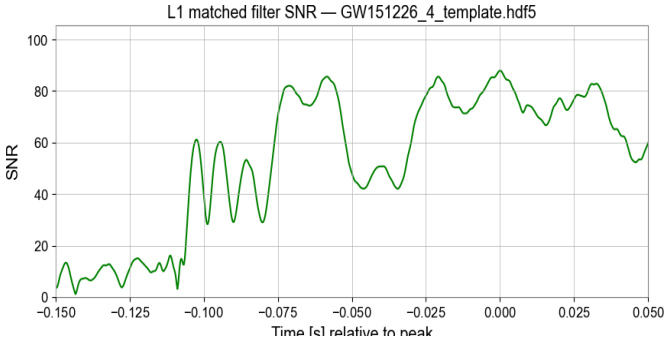

Figure 11. SNR time series for GW170817 using the GW151226 template.

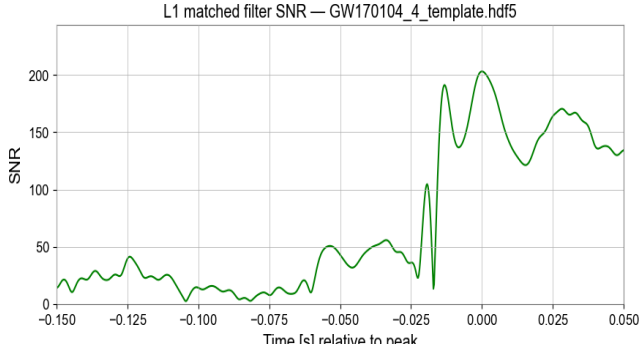

Figure 12. SNR time series for GW170817 using the GW170104 template.

4.2 GW150914: binary black hole merger

We next consider GW150914, the first directly detected binary black hole merger. Figure 13 shows its Q-transform. The chirp is much shorter and terminates at lower frequencies compared to GW170817, reflecting the higher masses of the black holes. The rapid chirp reflects the higher masses of the merging black holes.

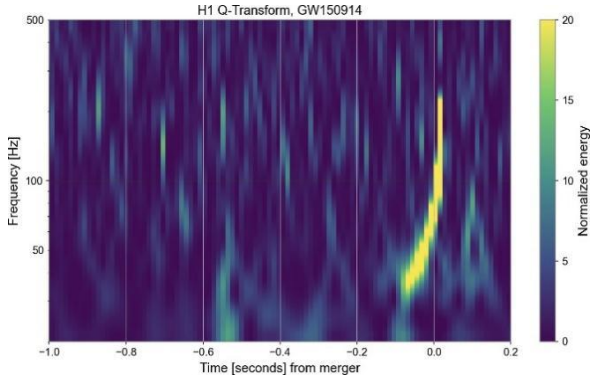

Figure 13. Q-transform of GW150914.

4.3 GW230627: binary black hole merger

We also analyzed GW230627, a confirmed gravitational-wave detection. Figure 14 shows the time- and frequency-domain, while Figure 15 presents the ASD.

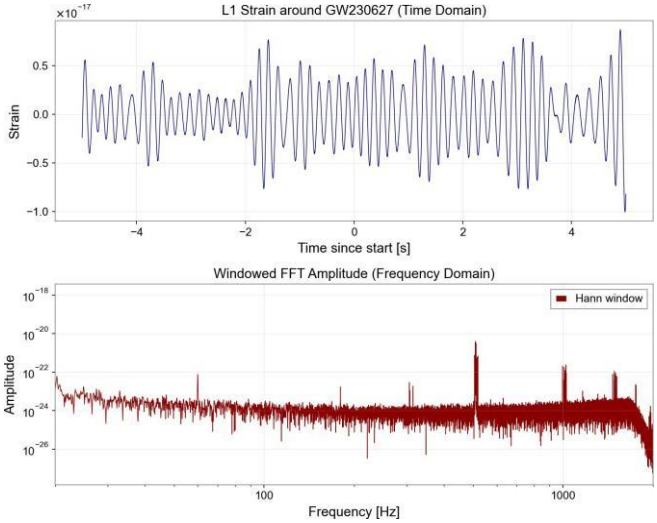

Figure 14. Time- and Frequency-domain spectrum of GW230627.

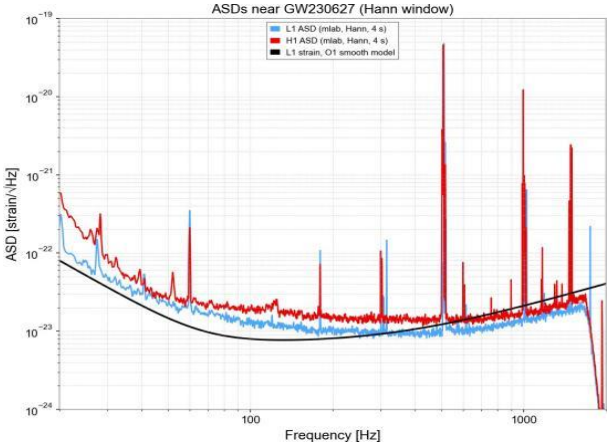

Figure 15. Amplitude spectral density (ASD) of GW170817.

Finally, the Q-transform in Figure 16 highlights the chirp-like track of the event, providing a clear visualization of the frequency evolution leading up to merger. The chirp is clearly visible as a rising track in frequency.

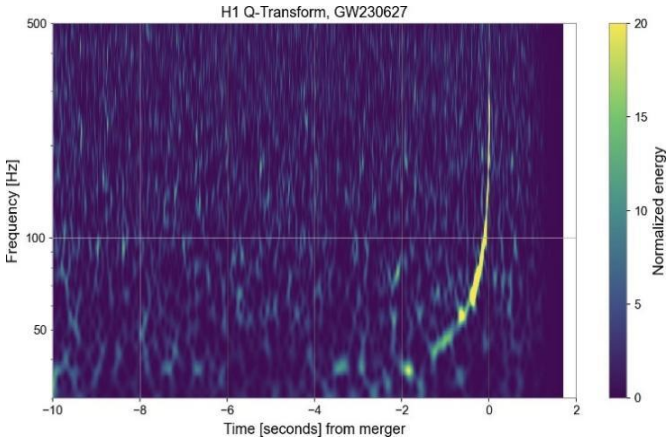

Figure 16. Q-transform of GW170817.

5. Discussion

Our analysis of GW170817, GW150914, and GW230627 demonstrates how gravitational-wave signals can be identified across multiple domains. GW170817's long inspiral was clearly visible in the time and

time–frequency analyses, while GW150914 showed a shorter, lower-frequency chirp consistent with heavier black holes. GW230627, a more recent detection, exhibited features consistent with a compact binary coalescence.

The complementary use of time-domain, frequency-domain, spectrogram, and Q-transform methods proved essential. Whitening and matched filtering further enhanced the signals, with SNR peaks confirming the presence of chirps. These results highlight both the robustness of gravitational-wave detections and the accessibility of open data for scientific exploration.

6. Conclusion

We successfully reproduced the characteristic chirp signals of three gravitational-wave events using open LIGO data. The results illustrate the differences between binary neutron star and binary black hole mergers, and confirm the consistency of more recent detections with established phenomenology.

7. Future Prospect

Looking forward, several directions can extend this work:

- **Refined GW recoil/kick modeling:** Extend numerical relativity studies to map recoil velocity dependence on spin geometry, mass ratio, and horizon curvature multipoles.
- **Plasma–GW interactions:** Investigate how magnetized plasma in post-merger environments (e.g., neutron star remnants or black hole–torus systems) modifies GW emission and couples to electromagnetic counterparts.
- **Numerical analysis:** Incorporate more advanced numerical techniques and high-performance computing to improve the resolution and accuracy of waveform modeling and data analysis.
- **Expanding event catalogs:** As more detections become available through GWOSC, sys- tematic comparisons across a growing population of events will enable deeper astrophysical insights and more stringent tests of general relativity.

8. Data Availibility

the gravitational-wave data used in this study are publicly available. All strain data and event information are provided by the Gravitational Wave Open Science Center (GWOSC) at https://gwosc.org/ [17], which hosts open releases from the LIGO, Virgo, and KAGRA collaborations. The most recent release, covering the first part of the fourth observing run (O4a), is described in Open Data from LIGO, Virgo, and KAGRA through the First Part of the Fourth Observing Run [18]. Reproducible workflows and example analyses are available through the LOSC Event Tutorial on GitHub [19], which demonstrates how to access and process open LIGO data.

Acknowledgments

I am deeply grateful to Prof. Mario Campanelli (University College London) for his invaluable guidance and support in my study of gravitational-wave data analysis. His mentorship strengthened my technical skills, deepened my understanding of compact binary coalescences, and inspired me to pursue further research in gravitational-wave astrophysics.

References

[1] Newton I. Philosophiae Naturalis Principia Mathematica. 2nd ed. London: Streater; 1713.

[2] Newton I. Philosophiae Naturalis Principia Mathematica. 1st ed. London: Streater; 1687.

[3] Misner CW, Thorne KS, Wheeler JA. Gravitation. San Francisco: Freeman; 1973.

[4] Einstein A. On the electrodynamics of moving bodies. Annalen der Physik. 1905;17:891.

[5] Einstein A. On the general theory of relativity. Sitzungsberichte der Preußischen Akademie der Wissenschaften. 1915:778–799.

[6] Einstein A. On the field equations of gravitation. Sitzungsberichte der Preußischen Akademie der Wissenschaften (Math. Phys.). 1915:844.

[7] Schutz BF. Gravitational waves on the back of an envelope. Am J Phys. 1984;52:412.

[8] Einstein A. Approximative integration of the field equations of gravitation. Sitzungsberichte der Preußischen Akademie der Wissenschaften Berlin (Math. Phys.). 1916:688.

[9] Einstein A. On gravitational waves. Sitzungsberichte der Preußischen Akademie der Wissenschaften Berlin (Math. Phys.). 1918:154.

[10] Hulse RA, Taylor JH. Discovery of a pulsar in a binary system. Astrophys J. 1975;195:L51.

[11] Kelley LZ. Pulsar Timing Arrays. arXiv preprint arXiv:2505.00797. 2025.

[12] Einstein Telescope [Internet]. Aei.mpg.de; 2015 [cited 2025]. Available from: https://www.aei.mpg.de/et

[13] Cosmic Explorer [Internet]. Einstein-Online.info; 2025 [cited 2025]. Available from: https://cosmicexplorer.org

[14] Comparison of global networks of third-generation gravitational-wave detectors. arXiv preprint arXiv:2411.05754. 2020.

[15] Abbott BP, et al. GW150914: First results from the search for binary black hole coalescence with Advanced LIGO. Phys Rev D. 2016;93:122003.

[16] Abbott BP, et al. Multi-messenger observations of a binary neutron star merger. Astrophys J. 2017;848:L12.

[17] Gravitational Wave Open Science Center (GWOSC) [Internet]. [cited 2025]. Available from: https://gwosc.org

[18] LOSC Event Tutorial [Internet]. GitHub; 2015 [cited 2025]. Available from: https://github.com/gwosc-tutorial/LOSCEvent_tutorial/blob/master/LOSCEvent_tutorial.ipynb

[19] LIGO Scientific Collaboration, Virgo Collaboration, KAGRA Collaboration. Open data from LIGO, Virgo, and KAGRA through the first part of the fourth observing run. arXiv preprint arXiv:2508.18079. 2023.